

Mid-Infrared (Mir) Light Guide Using Negative Curvature Hollow Core Fibers

Jannatul Ambia Akhi¹, Md Mehadi Hasan², Md Akramul Hossain³

Department of Electrical and Electronic Engineering, North Western University, Khulna, Bangladesh

Abstract: The use of mid-infrared fiber in the 2–12 μm spectral range has been widespread in a variety of application areas, including nonlinear optics, telecommunications, medical, and the military. Night vision, surveillance, and missile guidance are some of the military uses. Mid-infrared fiber lasers have advanced significantly over the past few decades thanks to advancements in pumping regimes, fiber components, and other associated technologies, and progressively caught up to or even surpassed classical lasers in some lasing performance. The confinement loss spectra of mid-infrared fiber spanning the wavelength range of 2 μm to 12 μm were simulated and examined using COMSOL Multiphysics. The study of confinement loss spectra is found that the high-loss and low-loss bands predicted by the ARROW surface model corresponded well with the confinement loss spectra regardless of the jack tube thickness, number of capillaries, core diameter, and wavelength. Three lowest order fundamental modes (TE_{01} , TM_{01} and HE_{11}) are considered and it is shown that the losses are minimum for all the cases. The designed fiber is very helpful to guide MIR light with low loss.

Keywords: Hollow-core Fiber (HCF), Negative Curvature HCF (NCHCF), TE Mode, TM Mode and HE Mode.

Date of Submission: 21-05-2023

Date of Acceptance: 01-06-2023

I. Introduction

The use of mid-infrared fiber lasers has significant advantages for both fundamental research and industry applications, such as telecommunications, remote sensing, molecular detection, mid-infrared supercontinuum generating, material processing, laser surgery, and biomedicine [1] [2] [3] [4]. Many molecular solids, liquids, and gas absorption bands appear in the mid-infrared region [4], [5]. At wavelengths of 2.9 μm , 2.8 μm , and 2.4 μm , respectively, strong absorption lines are evident for the atmospheric constituents NO_2 , CO_2 , and CO . Since these transmission wavelengths are available, mid-infrared fiber lasers can be used in the telecommunications and remote sensing industries. On the other hand, these mid-infrared fiber lasers can be employed for molecular detection. In their mid-infrared absorption spectra, the majority of polymer materials exhibit a noticeable absorption band about 3.4 μm [6] [7].

The term "IR optical fibers" refers to materials that can carry both MIR and FIR radiation with wavelengths between 2 μm to 25 μm . The first chalcogenide glass (ChG) fiber made from the IR glass arsenic trisulfide (As_2S_3) was described in the middle of the 1960s, ushering in a lengthy and fascinating history for these fibers. It is exciting that IR fibers have made substantial strides in each of these areas, as this bodes well for a potential mass adoption in the future [6], [8] and [9].

Mid-infrared fiber lasers that operate in this frequency range can be utilized to treat polymer compounds. Furthermore, a lot of plastic materials have enough absorption at a wavelength of 2 μm to permit direct processing with mid-infrared fiber lasers at this wavelength [8]. The mid-infrared fiber lasers at 2 μm and 3 μm are suitable options for laser surgery and biomedical applications, such as photo dermatology [9] and tissue ablation [10]

Due to the high water content of biological tissue, there are strong absorption lines at 2 μm and 3 μm . Applications in the military, including night vision, surveillance, and missile guidance (at wavelengths of 8–12 μm) and There is a lot of interest in the research field due to the large variety of applications for mid-infrared fiber lasers. The employment of silica optical fibers for the transmission of CO_2 laser beams, military applications like missile guidance, night vision, and surveillance, is restricted by the mid-IR spectrum (in this study, we define the spectrum between 2 and 12 μm) material loss of silica-based glasses. Negative curvature hollow-core fibers (NCHCFs) have recently drawn attention for their low loss transmission and wide bandwidth in applications such as high-power light delivery, gas-light interaction in restricted spaces, and mid-IR navigation [11][12] [13],[14],[15]. Since air is normally transparent to IR radiation, a hollow-core silica fiber can be employed as a low-loss medium for the mid-IR range [17], [18], and [19]. However, at wavelengths greater than 4.5 μm , the transmission loss of silica NCFs becomes considerable due to the significant rise in silica's absorption. Alternative mid-IR transparent materials, including as chalcogenide and fluoride glasses, are chosen for building NCFs in the mid-IR range. [16], [17], [18].

In conventional fiber, the core has a higher refractive index than the cladding. Because of total internal reflection (TIR), light can be entirely trapped within the fiber core. TIR, however, is unable to adequately capture the spreading processes in the case of the leaky fiber. Even leaky fibers with photonic band gaps in their claddings, such as band-gap fibers, exhibit loss as a fundamental property. [19]. The ARROW model, which stands for Anti-Resonant Reflecting Optical Waveguide, is commonly used to describe the properties of hollow core fibers with photonic band gaps and other hollow-core fibers. According to this theory, the layer with the high refractive index resembles a Fabry-Perot cavity. Light emerges from the layer with a high refractive index when the wavelength is close to the resonant wavelength. When the propagating wavelength is far from the resonant wavelength, however, the light should be reflected back, resulting in good confinement. As a result, the necessity for wavelength matching determines the band boundaries of high-loss and low-loss zones [19].

The term negative curvature hollow core fiber (NCHCF) has two separate nomenclatures: negative curvature and hollow core fiber. The light guides in a HCF through the air core. The cladding regions are made of higher indexed material like silica, PMMA etc. It has been found that more than 98% of the mode is confined in air which makes the fibers very radiation insensitive and suitable for radiation hard environments [20]. The cladding region can be made of micro structured air holes [21],[22] or single ring tube structured [23], [24] or solid [25]. The hollow core fiber provides 30% faster communication, allows higher bandwidth and zero polarization effect due to low material absorption loss of air core [19].

For the production of km-long fibers utilizing a number of methods, chalcogenide glasses are appropriate [26], [27] and in the mid-IR region, both of which have huge transmission windows and minimal optical losses. Several chalcogenide NCFs that steer the light using the principle of blocked coupling have been proposed for low-loss CO₂ laser delivery [28], [29]. A recently proposed NCF with a single ring of identical tubular cladding pieces encircling the hollow core has garnered interest because of its low-loss light direction and unobtrusive look [30]. Future research revealed that increasing the number of elements in the cladding structure greatly lowers losses because it improves light confinement [20], [31]. To the best of knowledge, chalcogenide NCFs with hybrid cladding structures have not been investigated in the mid-IR spectrum; however, NCFs with tubular, elliptical, and nested-cladding components have been investigated in the near-IR region [20],[31] and [32]. By conducting systematic research on identical and hybrid cladding designs, it is possible to increase the design alternatives for the mid-IR guidance.

This study will investigate how light transmits with low loss via fibers using the mode analysis in RF modules as the electromagnetic model. Setting the proper boundary conditions and meshing will affect how accurately the confinement loss will perform. Our main focus is on the confinement loss spectra, which are affected by a lot of factors, such as the wavelength, the number of capillaries, the capillary thickness, the core size, and so on.

II. Fiber Design And Modeling

The performance of a hollow core fiber with an air core embedded with ten capillaries and a dielectric cladding was studied in this work for a range of system parameters, including wavelengths, core diameter, jack tube thickness, number of capillaries, and their thickness. Using Comsol Multiphysics TM, the NCHCF system model is illustrated in two dimensions. Silica glass is utilized in the study as a capillary and jack tube material. In Fig. 1, where the design data is given, the suggested fiber system's cross-section is depicted. The design includes an air core with a diameter of D , jack tubes with a thickness of T , capillaries with a number N , inner diameter of d_{in} , capillaries with a thickness of t , and fibers with a diameter of D_f . The basic design parameters that were employed in the simulation are listed in Table 1.

The following formula is used to calculate the confinement loss (CL) in dB/m [33].

$$C_L = 8.686 \left(\frac{2\pi}{\lambda} \right) \cdot \text{Im}(n_{eff}) \text{ dB/m} \quad (1)$$

In this equation, $\text{Im}(n_{eff})$ is the imaginary part of the effective refractive index, and λ is the incident wavelength. The refractive index of the cladding dielectric, which is made of silica, can be changed using the Sellmire equation [34].

$$n^2(\lambda) = 1 + \frac{B_1\lambda^2}{\lambda^2 - c_1} + \frac{B_2\lambda^2}{\lambda^2 - c_2} + \frac{B_3\lambda^2}{\lambda^2 - c_3} \quad (2)$$

where the values of the Sellmire constants, B_1 , B_2 , B_3 , C_1 , C_2 , and C_3 , are, respectively, 0.696163, 0.4079426, 0.897479400, 0.0046791486, 0.0135120631, and 97.9340025.

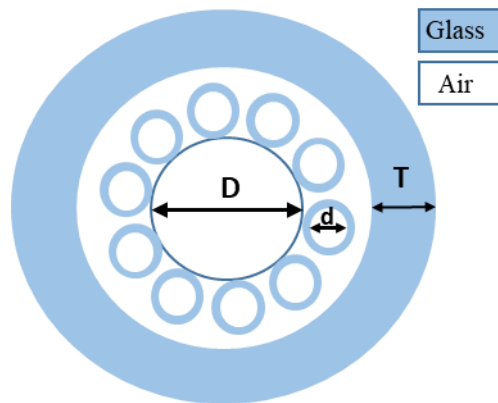


Fig. 1: 2D cross-sectional image of the proposed hollow core fiber exhibiting the design data.

Table No. 1: Proposed system design parameters for an IR application Fiber.

Name	Value	Expression
D	119[μm]	Diameter of the fiber core
N	10	Number of capillaries
d_{in}	51[μm]	Inner diameter of capillary
t	6[μm]	Thickness of capillary
T	35[μm]	Thickness of jack tube
D_f	315[μm]	Diameter of the fiber

III. Result and Discussion

Three lowest order modes were taken into account for simplifying the analysis. Here, we take into account that the entering light's electric field changes in the x-direction while the wave moves in the z-direction. The lowest order mode of a waveguide is another definition for the fundamental mode. Here, LP_{01} , which is the same as HE_{11} , has been chosen as the fundamental mode. To observe the loss components of the organized fiber, we also took into account two additional low loss modes, LP_{11} odd (equal to TE_{01} or HE_{21} odd) and LP_{11} even (corresponding to TM_{01} or HE_{21} even). Fig. 2 displays schematic illustrations of the electric field distribution for the modes taken into consideration in this work.

Effects of Wavelength

The loss spectra between 2 μm and 12 μm wavelength is investigated with $D = 119 \mu\text{m}$, $d_{out} = 63 \mu\text{m}$, $d_{in} = 51 \mu\text{m}$, $T = 35 \mu\text{m}$. Fig. 3 depicts the outcome. The loss spectra that ranges (10^{-14} dB/m to 10^{-11} dB/m) is found for MIR light guide. All three considered fundamental modes (TE_{01} , TM_{01} and HE_{11}) losses are minimum. HE_{11} mode loss is the lowest one than others. Minimum loss is found at 7 μm wavelength for TM_{01} mode.

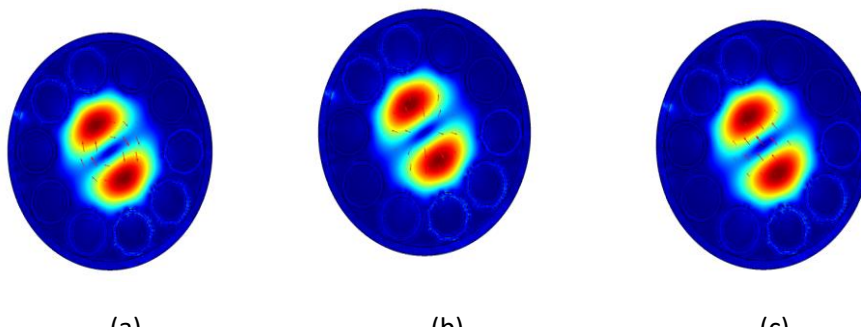


Fig. 02: Electric Field Distribution profile of (a) TE_{01} , (b) TM_{01} and (c) HE_{11} modes

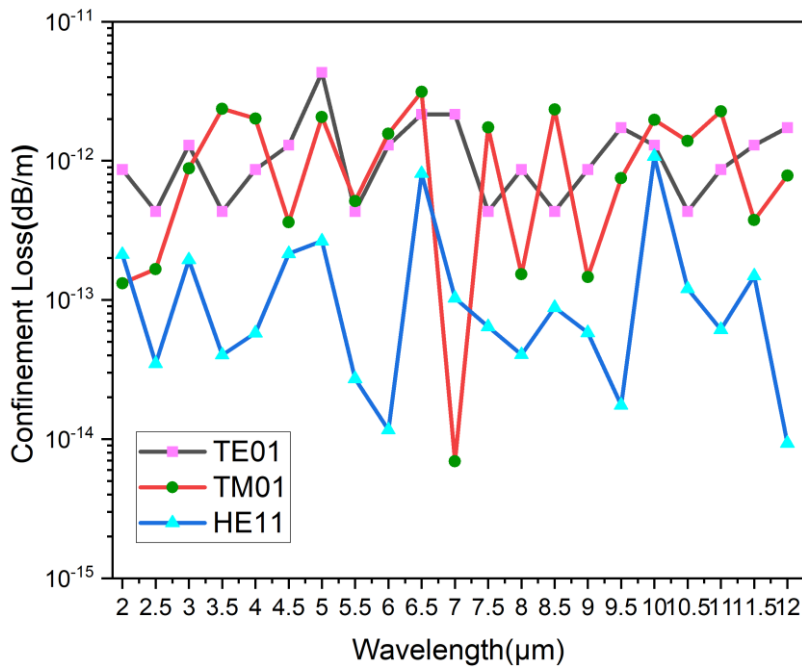


Fig. 3: Confinement loss spectra with wavelengths.

This 7μm wavelength is remain fixed for considering the effect of different design parameters like (size of the core, thickness of the jack tube, and the number of capillaries). Because of this low loss, these wavelength ranges are also becoming more and more important in military applications including missile guidance, night vision, surveillance, satellite detection, space observation, and space vehicle navigation and flight control.

Effects of core diameter

The outcome (Fig. 4) demonstrates that confinement loss drastically decreases when core diameter is varied from 100 to 200 μm, where loss is steadily lowered. Large core diameter optical fiber can attempt multimodal light guidance in the fiber core, including the basic and higher order modes. High confinement loss caused by multimodal guiding in the large core fiber had an impact on high-order mode loss and bending loss. But, in this study, the losses are minimum for all three considered modes and lowest loss is found for TM₀₁ modes.

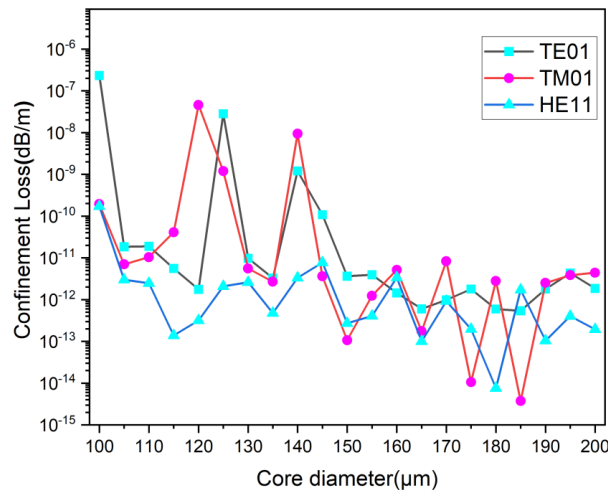


Fig. 4: Confinement loss spectra with various core diameters

Effects of the thickness of jack tube

When the thickness of the jack tube T changes, the wavelength of the fiber remains constant. Fig. 5 depicts the outcome. Fig. 5 demonstrates how confinement loss rapidly decreases as jack tube thickness increases. TE_{01} mode loss is higher than others. When jack tube thickness is $55\mu\text{m}$, HE_{11} mode loss is minimum.

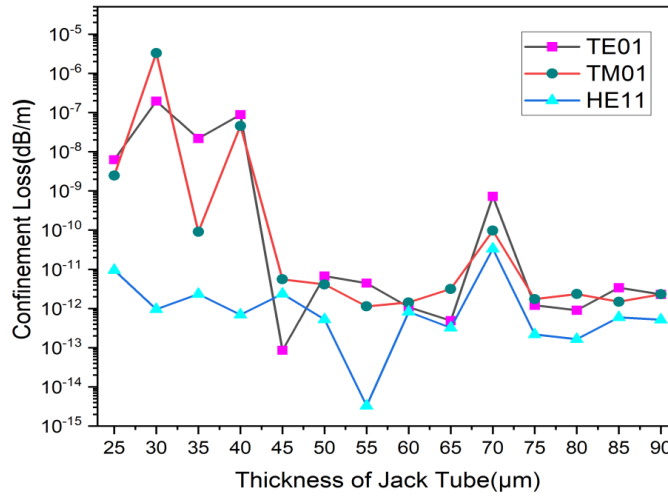


Fig. 5: Confinement loss spectra for jack tubes of various thicknesses

Effect of no of capillaries

The variation of confinement loss with no of capillary is shown in fig. 6. Here, $D = 119\mu\text{m}$, $d_{out} = 63\mu\text{m}$, $d_{in} = 51\mu\text{m}$, $T = 35\mu\text{m}$ are considered. While the number of capillaries N changes, the fiber's wavelength λ remains constant. Confinement loss gradually decreases as the number of capillaries increases. HE_{11} mode exhibits the lowest loss than others. But, when capillary no is 10, HE_{11} mode exhibits the highest loss and minimum losses are found when the capillary no is 24.

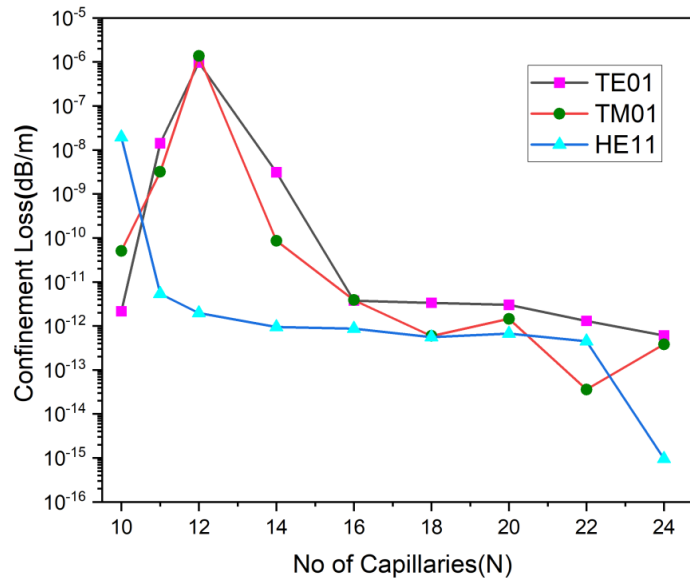


Fig. 6: Confinement loss spectra with different no of capillaries

IV. Conclusion

In this study, we design and investigate the performance of NCHCFs to guide MIR light ($2\mu\text{m} - 12\mu\text{m}$) with low losses considering three fundamental modes (TE_{01} , TM_{01} and HE_{11}). COMSOL Multiphysics is used to simulate and examine the confinement loss spectra of this mid-infrared fiber. The effects of wavelength, capillary thickness, no of capillary, and fiber core diameter on confinement loss are also examined. The findings

of this research could aid in the design of mid-infrared fiber for military applications such as missile guidance, night vision, surveillance, space observation, space vehicle navigation, and flight control with relatively low losses.

References

- [1] J. Mandon, G. Guelachvili, and N. Picqué, "Fourier transform spectroscopy with a laser frequency comb," *Nat. Photonics*, vol. 3, no. 2, pp. 99–102, 2009, doi: 10.1038/nphoton.2008.293.
- [2] D. D. Hudson et al., "Toward all-fiber supercontinuum spanning the mid-infrared," *Optica*, vol. 4, no. 10, p. 1163, 2017, doi: 10.1364/optica.4.001163.
- [3] S. D. Jackson, "Towards high-power mid-infrared emission from a fibre laser," *Nat. Photonics*, vol. 6, no. 7, pp. 423–431, 2012, doi: 10.1038/nphoton.2012.149.
- [4] M. Ebrahim-Zadeh and I. T. Sorokina, "Mid-Infrared Coherent Sources and Applications: Preface," *NATO Sci. Peace Secur. Ser. B Phys. Biophys.*, vol. 33, no. 11, p. 3224, 2008.
- [5] Z. Qin et al., "Black phosphorus Q-switched and mode-locked mid-infrared Er:ZBLAN fiber laser at 35 μm wavelength," *Opt. Express*, vol. 26, no. 7, p. 8224, 2018, doi: 10.1364/oe.26.008224.
- [6] C. Frayssinous, V. Fortin, J. P. Bérubé, A. Fraser, and R. Vallée, "Resonant polymer ablation using a compact 3.44 μm fiber laser," *J. Mater. Process. Technol.*, vol. 252, no. April 2017, pp. 813–820, 2018, doi: 10.1016/j.jmatprotec.2017.10.051.
- [7] K. Scholle, S. Lamrini, P. Koopmann, and P. Fuhrberg, 2010 - *Frontiers in Guided Wave Optics and Optoelectronic - 2 μm laser sources and their possible applications.pdf*, no. February 2010.
- [8] G. Tao et al., "Infrared fibers," vol. 458, pp. 379–458, 2015, doi: 10.1364/AOP.
- [9] J. D. Shephard, W. N. Macpherson, R. R. J. Maier, J. D. C. Jones, and D. P. Hand, "Single-mode mid-IR guidance in a hollow-core photonic crystal fiber," vol. 13, no. 18, pp. 11–16, 2005.
- [10] L. Ha et al., "First Assessment of a Carbon Monoxide Laser and a Thulium Fiber Laser for Fractional Ablation of Skin," *Lasers Surg. Med.*, vol. 52, no. 8, pp. 788–798, 2020, doi: 10.1002/lsm.23215.
- [11] A. N. Kolyadin, A. F. Kosolapov, A. D. Pryamikov, A. S. Biriukov, V. G. Plotnichenko, and E. M. Dianov, "Light transmission in negative curvature hollow core fiber in extremely high material loss region," *Opt. Express*, vol. 21, no. 8, p. 9514, 2013, doi: 10.1364/oe.21.009514.
- [12] Y. Y. Wang, N. V. Wheeler, F. Couny, P. J. Roberts, and F. Benabid, "Low loss broadband transmission in hypocycloid-core Kagome hollow-core photonic crystal fiber," *Opt. Lett.*, vol. 36, no. 5, p. 669, 2011, doi: 10.1364/ol.36.000669.
- [13] F. Yu, W. J. Wadsworth, and J. C. Knight, "Low loss silica hollow core fibers for 3–4 μm spectral region," *Opt. Express*, vol. 20, no. 10, p. 11153, 2012, doi: 10.1364/oe.20.011153.
- [14] Z. Zhou et al., "High-power tunable mid-infrared fiber gas laser source by acetylene-filled hollow-core fibers," *Opt. Express*, vol. 26, no. 15, p. 19144, 2018, doi: 10.1364/oe.26.019144.
- [15] F. B. A. Aghbolagh et al., "Mid IR hollow core fiber gas laser emitting at 46 μm ," *Opt. Lett.*, vol. 44, no. 2, p. 383, 2019, doi: 10.1364/ol.44.000383.
- [16] C. Wei, J. Hu, and C. R. Menyuk, "Comparison of loss in silica and chalcogenide negative curvature fibers as the wavelength varies," *Front. Phys.*, vol. 4, no. JUL, pp. 1–10, 2016, doi: 10.3389/fphy.2016.00030.
- [17] R. Kitamura et al., "Optical constants of silica glass from extreme ultraviolet to far infrared at near room temperature," *Water Res.*, vol. 53, no. 1, pp. 1–8, 2020, [Online].
- [18] J. Bei, T. M. Monro, A. Hemming, and H. Ebendorff-Heidepriem, "Fabrication of extruded fluorindate optical fibers," *Opt. Mater. Express*, vol. 3, no. 3, p. 318, 2013, doi: 10.1364/ome.3.000318.
- [19] J. M. Senior, *Optical Fiber Communications*.
- [20] F. C. Meng, B. W. Liu, Y. F. Li, C. Y. Wang, and M. L. Hu, "Low Loss Hollow-Core Antiresonant Fiber with Nested Elliptical Cladding Elements," *IEEE Photonics J.*, vol. 9, no. 1, pp. 1–11, 2017, doi: 10.1109/JPHOT.2016.2639044.
- [21] R. Buczynski, "Photonic Crystal Fibers," vol. 106, no. 2, pp. 141–167, 2004.
- [22] C. H. W. E. R. J. O. W. Eiblen, and C. U. R. M. Enyuk, "Negative curvature fibers," vol. 9, no. 3, pp. 504–561, 2017.
- [23] H. I. Stawska, D. Elektronen-synchrotron, and M. Popena, "nt Hollow Core Fibers with Core Fibers with Modified Shape Core Performance for the Better Optical Performance Core for the the Visible Spectral Region — A Numerical Study e Spectral in Region — A Numerical," no. August, 2018, doi: 10.3390/polym10080899.
- [24] W. Ding and Y. Wang, "Semi-analytical model for hollow-core anti-resonant fibers," vol. 3, no. March, pp. 1–12, 2015, doi: 10.3389/fphy.2015.00016.
- [25] W. Ding, Y. Y. Wang, S. F. Gao, M. L. Wang, and P. Wang, "Recent Progress in Low-Loss Hollow-Core Anti-Resonant Fibers and Their Applications," *IEEE J. Sel. Top. Quantum Electron.*, vol. 26, no. 4, 2020, doi: 10.1109/JSTQE.2019.2957445.
- [26] B. Zhang et al., "Low loss, high Na chalcogenide glass fibers for broadband mid-infrared supercontinuum generation," *J. Am. Ceram. Soc.*, vol. 98, no. 5, pp. 1389–1392, 2015, doi: 10.1111/jace.13574.
- [27] R. R. Gattass et al., "Infrared glass-based negative-curvature anti-resonant fibers fabricated through extrusion," *Opt. Express*, vol. 24, no. 22, p. 25697, 2016, doi: 10.1364/oe.24.025697.
- [28] J. Tu et al., "Chalcogenide-glass nested anti-resonant nodeless fibers in mid-infrared region," *J. Light. Technol.*, vol. 36, no. 22, pp. 5244–5253, 2018, doi: 10.1109/JLT.2018.2870434.
- [29] A. D. Pryamikov, A. S. Biriukov, A. F. Kosolapov, V. G. Plotnichenko, S. L. Semjonov, and E. M. Dianov, "Demonstration of a waveguide regime for a silica hollow - core microstructured optical fiber with a negative curvature of the core boundary in the spectral region > 35 μm ," *Opt. Express*, vol. 19, no. 2, p. 1441, 2011, doi: 10.1364/oe.19.001441.
- [30] F. Poletti, "Nested antiresonant nodeless hollow core fiber," *Opt. Express*, vol. 22, no. 20, p. 23807, 2014, doi: 10.1364/oe.22.023807.
- [31] M. S. Habib, O. Bang, and M. Bache, "Low-loss single-mode hollow-core fiber with anisotropic anti-resonant elements," *Opt. Express*, vol. 24, no. 8, p. 8429, 2016, doi: 10.1364/oe.24.008429.
- [32] S. Chaudhuri, L. D. Van Putten, F. Poletti, and P. J. A. Sazio, "Low Loss Transmission in Negative Curvature Optical Fibers with Elliptical Capillary Tubes," *J. Light. Technol.*, vol. 34, no. 18, pp. 4228–4231, 2016, doi: 10.1109/JLT.2016.2598491.
- [33] A. Kajla and S. Gupta, "Evaluation of Confinement Loss of Different," vol. 3, no. 2, pp. 1521–1525, 2014.
- [34] H. N. Rafi, R. Kaysir, and J. Islam, "Sensing and Bio-Sensing Research Air-hole attributed performance of photonic crystal fiber-based SPR sensors," *Sens. Bio-Sensing Res.*, vol. 29, no. June, p. 100364, 2020, doi: 10.1016/j.sbsr.2020.100364.